The Bend: Origin and Significance by Rex H. Pilger

Data Repository: Tables and Appendix

Table 1: Reconstruction Pairs, Magnetic Chrons, Parameter Sources

Plate or Hotspot-Plate Pair	**Set***	**Magnetic Chrons or *[Ages, Ma]*** (Cande et al., 1995, time scale)	**Parameter Source(s)**
Eurasian > North American		5, 6, 13, 21, 24, 25, 31, 33o, 34y	Müller et al. (1997)†
North American > African	A	5y, 6y, 8y, 13y, 18y, 21y, 24y, 25y, 30y, 32n2y, 33o, 34y	Müller et al. (1999)
	B	5, 6, 13, 21, 25, 30, 32, 33y, 33o, 34y	Müller et al. (1997)†
South American > African	C	5y, 6y, 8y, 13y, 18y, 21y, 24y, 25y, 30y, 32n2y, 33o, 34y	Müller et al. (1999)
	D	1o, 2, 2A, 3, 3A, 4, 4A, 5, 5A-5E, 6, 6A-C, 7-13, 15-33, 33R, 34y	Cande and Kent (1988)
African > East Antarctic	E	5, 6, 13, 20, 21, 23, 25, 28, 32, 33, 34y	Norton (2000)†
	F	5, 6, 13y, 18, 20, 22, 24, 28y, 31y, 33, 34y	Müller et al. (1997)†
East Antarctic > West Antarctic		9o (no subsequent motion), 13o, 20o	Cande et al. (2000)
West Antarctic > Pacific	G‡	2Ay, 3Ay, 5o, 6o, 8o, 13o	Cande and Stock (2004)
	H	2Ay, 3Ay, 4Ay, 5A, 5D, 6Cn3, 10y, 13o, 20y, 21o, 24o, 27, 31y, 32, 33o, 34y	Norton (2000)†
East Antarctic > Australian	I‡	2Ay, 3Ay, 5o, 6o, 8o, 13o	Cande and Stock (2004)
	J	5, 6, 13y, 18, 20, 24, 31y, 33o, 34y	Müller et al. (1997)†
Pacific > Farallon		5, 6, 13	Norton (1995)

Pacific > Vancouver		18, 21, 25, 30r, 32, 34y	Norton (1995) combined with Rosa and Molnar (1988)
Pacific > Nazca		1o, 2a, 3a, 4a, 5o, 5AA, 5B, 5D, 6C, 7y, 10y 13, 18, 21, 25, 32, 34y	Wilder (2003) Mayes et al. (1990)
Hawaiian hotspot frame > Pacific**		*[5, 10.83, 21.16, 25, 33.3, 40.22, 43, 43.87, 47.86, 53.25, 63.3, 68.68, 78.78]*†† *[25,43,81,90]* *[2-70], at 2 m.y. intervals*	Raymond et al. (2000, corrected) Norton (2000) Harada and Hamano (2000)
Pacific > Farallon & Pacific>Vancouver		5, 6, 13 18, 21, 25, 30r, 32, 34y	Norton (1995) Norton (1995) combined with Rosa and Molnar (1988)
Tristan hotspot frame > African		5o, 13y, 18o, 21o, 25y, 31y, 33y, 33o, 34y	Müller et al. (1993)

* If more than one set is listed, preferred source is listed first. Second set is referred to in the Appendix.

† Compilation

‡ Chrons 18 through 34y for sets G and I from sets H and J, respectively

** Reconstruction ages were reassigned and linearly interpolated to modify the age of the Hawaiian-Emperor bend from 43 to 48 Ma. (e.g., Sharp and Clague, 2002). Reconstructions younger than 25 Ma were unmodified. Those from 25 to 43 Ma linearly interpolated to between 25 and 48 Ma. Reconstructions 43 Ma and older were linearly interpolated to between 48 Ma and the oldest reconstruction provided.

†† Raymond et al. associated the ages with magnetic chrons, but the published chrons and ages are not completely consistent with the time scales of either Cande and Kent (1992) or Cande and Kent (1995). Therefore the reported ages are used, without correction to the cited (Cande and Kent, 1995) time scale.

Table 2: Plate Circuits

Circuit	Plate Pair 1	Plate Pair 2	Resulting Plate Pair
1	E. Antarctic > W. Antarctic	W. Antarctic > Pacific	E. Antarctic > Pacific
2	African > East Antarctic	E. Antarctic > Pacific	African > Pacific
3	North American > African	African > Pacific	North American > Pacific
4	South American > African	African > Pacific	South American > Pacific
5	Eurasian > North America	American > Pacific	Eurasian > Pacific
6	Australian > East Antarctic	E. Antarctic > Pacific	Australian > Pacific

Table 3: Interpolated Reconstruction Parameters

	Total Rotation		
Age (Ma)	Longitude (ºE)	Latitude (ºN)	Angle (ºCCW)
Eurasia-North America			
5	-45.906	-63.528	1.111
10	-46.452	-65.227	2.349
15	-45.11	-67.635	3.72
20	-43.128	-68.935	5.073
25	-42.308	-67.923	6.141
30	-42.561	-66.109	6.967
35	-43.352	-65.909	7.831
40	-44.024	-67.726	8.98
45	-43.252	-68.204	10.335
50	-40.527	-64.511	11.735
55	-38.584	-62.779	13.709
60	-37.644	-64.011	15.537
65	-36.76	-64.57	16.511
70	-35.562	-65.013	17.207
75	-33.928	-65.599	18.072
80	-32.092	-66.225	19.099
North America-Africa			
5	45.656	79.624	1.164
10	49.921	80.059	2.354
15	46.051	80.003	3.814
20	34.5	79.479	5.533
25	18.717	78.182	7.194
30	5.938	76.314	8.839
35	-0.363	75.241	10.761
40	-2.205	75.29	12.941
45	-3.468	75.422	14.796
50	-3.622	76.41	16.261
55	-2.017	78.449	17.502
60	1.552	80.785	18.779
65	4.01	82.4	20.249
70	-2.698	82.259	21.931
75	-13.113	80.359	24.265
80	-18.664	78.127	27.347
South America-Africa			
5	-39.118	61.026	1.567
10	-38.651	59.722	3.29
15	-37.898	58.702	5.32
20	-36.981	57.887	7.589
25	-35.949	57.138	9.785

30	-34.755	56.669	11.937
35	-33.414	56.811	14.356
40	-32.309	57.532	16.932
45	-31.843	58.474	18.839
50	-31.519	59.475	20.311
55	-31.337	60.534	21.69
60	-31.916	61.803	23.1
65	-33.078	62.936	24.619
70	-33.69	63.212	26.254
75	-33.869	63.166	28.286
80	-34.228	62.789	31.322
East Antarctica-Africa			
5	15.441	21.906	2.496
10	14.751	23.017	4.89
15	9.025	25.781	7.017
20	4.724	27.344	9.116
25	9.101	25.546	11.51
30	16.589	22.743	14.471
35	20.623	22.41	17.723
40	19.055	23.4	20.763
45	14.381	21.09	23.976
50	11.722	18.801	27.898
55	11.291	17.567	32.751
60	10.364	15.849	38.834
65	8.896	14.162	45.376
70	7.605	13.527	50.597
75	6.424	13.764	54.203
80	6.128	13.205	58.484
East Antarctica-Australia			
5	35.978	14.469	3.169
10	34.03	15.461	6.229
15	32.801	15.85	9.227
20	32.751	15.313	12.217
25	33.802	13.948	15.266
30	34.301	13.176	18.373
35	32.395	14.601	21.44
40	29.726	16.736	23.86
45	30.583	15.902	24.483
50	31.809	14.126	24.642
55	31.735	12.805	25.127
60	31.876	11.32	25.529
65	32.609	9.65	25.743
70	33.504	8.288	25.872
75	34.308	7.334	26.034
80	35.189	6.044	26.421
East Antarctica-West Antarctica			
25	0	0	0

30	-17.847	-18.146	0.161
35	-17.847	-18.146	0.924
40	-17.847	-18.146	1.52
45	-17.847	-18.146	1.7
80	-17.847	-18.146	1.7
Pacific-West Antarctica			
5	-71.746	68.452	4.714
10	-75.345	70.512	8.954
15	-71.783	72.916	13.265
20	-68.252	74.303	17.142
25	-67.231	74.737	20.688
30	-67.219	74.418	24.296
35	-62.882	74.481	28.485
40	-53.488	74.889	33.214
45	-49.805	74.723	36.659
50	-50.977	74.212	38.652
55	-53.109	73.378	40.534
60	-55.329	72.011	43.426
65	-54.917	70.202	48.072
70	-52.029	68.84	53.11
75	-53.044	67.358	55.955
80	-54.501	66.01	59.076
Pacific-Nazca			
5	-89.734	59.192	6.21
10	-89.009	58.671	14.282
15	-90.116	60.589	22.97
20	-90.12	62.188	31.165
25	-90.667	63.047	39.663
30	-99.142	66.702	46.086
35	-104.796	70.771	51.762
40	-114.033	72.991	58.064
45	-123.42	73.876	64.815
50	-132.126	75.455	70.075
55	-141.029	77.653	73.14
60	-145.541	78.828	74.868
65	-145.437	79.082	76.534
70	-148.515	79.313	80.102
75	-163.326	79.898	87.664
80	-172.751	79.488	93.746
Pacific-Farallon			
5	54.68	72.94	3.11
10	55.422	72.558	6.28
15	58.106	71.221	9.22
20	58.423	72.686	12.75
25	52.076	78.468	18.628
30	41.041	83.324	26.743
35	44.513	85.497	34.859

40	65.602	85.588	41.261
45	72.943	85.766	46.847
50	85.395	85.362	51.649
55	98.758	83.956	55.732
60	104.797	82.837	59.302
65	107.255	82.354	62.322
70	108.866	82.088	64.76
75	110.695	81.29	68.839
80	112.294	79.835	76.13
Pacific-Vancouver			
5	54.734	72.829	3.106
10	55.431	72.539	6.278
15	58.014	71.522	9.251
20	58.449	72.602	12.738
25	53.116	77.283	18.318
30	44.046	82.295	26.258
35	39.865	86.342	35.446
40	79.98	89.389	44.205
45	-153.742	88.362	51.388
50	-178.609	87.488	56.69
55	146.454	86.012	60.596
60	135.403	84.609	64.028
65	133.429	84.021	67.086
70	132.486	83.653	69.555
75	129.468	82.764	73.617
80	125.765	81.292	80.903
Pacific-Hawaiian Hotspot Frame			
5	-75.1	56.5	4.7
10	-71.459	64.393	8.642
15	-69.833	70.207	12.388
20	-68.403	70.432	16.46
25	-67.56	71.2	20.49
30	-65.273	70.91	23.337
35	-62.791	69.342	25.22
40	-61.741	68.039	27.285
45	-59.738	67.938	29.915
50	-61.777	65.863	31.777
55	-66.166	62.177	33.566
60	-69.306	58.707	35.218
65	-71.702	55.494	37.253
70	-73.568	52.546	39.37
75	-73.668	51.065	39.894
80	-77.227	46.519	45.577
African-Tristan Hotspot Frame			
5	-0.641	47.218	0.71
10	-26.615	58.711	1.661
15	-42.815	57.085	2.946

20	-44.506	51.057	4.323
25	-44.196	45.752	5.74
30	-43.597	41.889	7.123
35	-42.508	39.599	8.379
40	-41.226	37.766	9.614
45	-40.706	34.575	11.171
50	-41.009	31.841	12.657
55	-41.623	30.318	13.72
60	-41.762	29.112	14.66
65	-41.313	27.576	15.644
70	-40.493	25.149	16.762
75	-39.173	20.9	18.293
80	-39.261	18.004	20.37

Appendix I - Reconstruction Combinations

Technique

The reconstructions for each plate pair from the sources in Table 1 were converted into pseudovector series as a function of time (using the time scale of Cande and Kent, 1995, for magnetic isochrons); the reconstruction poles were converted to unit vectors and to which the total rotation rate (total rotation angle divide by age of the reconstruction) was applied, producing the pseudovectors. For the present, the instantaneous models of DeMets et al. (1991) and Gripp and Gordon (1991), converted to the Cande and Kent (1995) time scale, were used.

Each pseudovector series was splined as a function of time (using the algorithm of Press et al., 1992), and interpolated at intervals of five m.y. Then the interpolated parameters (converted to quaternion parameters) were combined in sequence to derive reconstructions of the Eurasian, North and South American, and Australian plates relative to the Pacific plate. In addition, the parameters for reconstructions of the Antarctic and Farallon plates relative to the Pacific plate were splined and interpolated. The plate reconstruction circuits were as follows: Eurasian-North American-African-East Antarctic-West Antarctic-Pacific; North American-African-East Antarctic-West Antarctic-Pacific; South American-African-East Antarctic-West Antarctic-Pacific; and Australian-East Antarctic-West Antarctic-Pacific (Table 2). Table 3 lists the resulting calculated parameters for the preferred sources listed in Table 1 for reconstructions 80 Ma and younger.

From the combined reconstruction parameters, loci of motion of the various plates relative to the Pacific plate were calculated from inferred hotspot locations. For mapping purposes linear segments connect the reconstructed points in each locus.

Uncertainties

Published uncertainties for all of the plate pairs in the Eurasian, North American and South American to Pacific circuits do not yet exist. In particular, reconstruction parameters without uncertainties have been published for Eurasia-North America, Africa-East Antarctica (for reconstructions prior to Chron 18), and West Antarctica-Pacific (prior to Chron 18). Since the critical issue is the apparent change in Pacific plate motion relative to the Hawaiian hotspot and the North and South American plates at ~47-48 Ma, the absence of quantitative uncertainties for reconstructions older than Chron 18 (between African-East Antarctica and West Antarctica-Pacific) precludes quantitative evaluation of the calculated changes.

To evaluate the uncertainty in the reconstructions, in the absence of complete quantitative uncertainty information for all of the plate pairs, an alternative procedure was followed. Alternative reconstruction sets were used for each for five plate pairs: North American-African, South American-African, African-East Antarctic, West Antarctic-Pacific, and Australian-East Antarctic (as noted in Table 1). Combinations of these alternative sets produces eight different parameter sets for Eurasian-Pacific, North American-Pacific and South American-Pacific, four sets for Australian-Pacific, and two sets for West Antarctic-Pacific circuits.

Figure A-1 illustrates the various calculated loci from this alternative procedure. For the North and South American plates, in particular, reconstructed motions relative to the

Pacific plate exhibit abrupt bends for all eight calculated loci at ~45 Ma. Similarly, the loci for other plate pairs also preserve similar trends to the preferred reconstructions illustrated in Fig. 3 and 4.

This procedure provides only graphical illustration of the effects of variations in published reconstructions using differing data sets and techniques and is not a substitute for a more complete uncertainty analysis. However the results should provide some degree of qualitative confidence in the interpreted trends in the absence of complete quantitative uncertainties for all of the reconstruction parameters utilized.

Appendix Figure Caption

Figure A-1. Graphical model alternative analysis: Reconstructed loci of various plates (and Hawaiian hotspot) relative to Pacific plate, reconstructed at 5 m.y. intervals, anchored at the Hawaii. Black loci are preferred plate reconstructions relative to the adjacent Pacific plate; gray loci are alternates. Spread of loci for each plate-pair provides some insight into the reproducibility of the reconstructions. Table 1 in the data repository indicates the sources used for the plate-to-plate reconstructions. For Hawaiian hotspot-Pacific loci, the alternative models of Harada and Hamano (2000; circles), Norton (2000; squares), and Raymond et al. (2000; diamonds) were used, recalibrated to an age of the bend of 48 Ma. Note that in all cases (especially for the North and South American plates), distinct changes in orientation of motion relative to the Pacific plate are observed near 45 Ma. If a finer interpolation were provided, the changes would be near 47 or 48 Ma. Magnetic isochrons and plate boundaries from Müller et al. (1997).

Supplementary References

Cande, S. C., LaBrecque, J. L., and Haxby, W. F. (1988) Plate kinematics of the South Atlantic: Chron 34 to present, Journal of Geophysical Research, v. 93, p. 13479-13492.

Cande, S. C., and Kent, D. V. (1992) A new geomagnetic time scale for the Late Cretaceous and Cenozoic, Journal of Geophysical Research, v. 97, p. 13917-13951.

Cande, S. C., and Kent, D. V. (1995) Revised calibration of the geomagnetic time scale for the Late Cretaceous and Cenozoic, Journal of Geophysical Research, v. 100, p. 6093-6095.

Cande, S. C., Raymond, C. A., Stock, J. M., and Haxby, W. F. (1995) Geophysics of the Pitman Fracture Zone and Pacific-Antarctic plate motions during the Cenozoic, Science, v. 270, p. 947-953.

Cande, S. C., Stock, J. M., Müller, R. D., and Ishihara, T. (2000) Cenozoic motion between East and West Antarctica, Nature, v. 404, p. 145-150.

Cande, S. C., and Stock, J. M. (2004) Pacific-Antarctic-Australia motion and the formation of the Macquarie plate, Geophysical Journal International, v. 157, p. 399-414.

Gripp, A. E., Gordon, R. G. (1991) Current plate velocities relative to the hotspots incorporating the NUVEL-1 global plate motion model, Geophysical Research Letters, v. 17, p. 1109-1112.

Harada, Y., and Hamano, Y. (2000) Recent progress on the plate motion relative to hotspots, *in* Richards, M. A., Gordon, R. G., and van der Hilst, R. D., editors, The history and dynamics of global plate motions, American Geophysical Union Geophysical Monograph 121, p. 327-338.

Mayes, C. L., Lawver, L. A., Sandwell, D. T. (1990) Tectonic history and new isochron chart of the South Pacific, Journal of Geophysical Research, v. 95, 8543-8567.

Müller, R. D., Royer, J.-Y., and Lawver, L. A. (1993) Revised plate motions relative to the hotspots from combined Atlantic and Indian Ocean hotspot tracks, Geology, v. 21, p. 275-278.

Müller, R.D., Roest, W.R., Royer, J.-Y., Gahagan, L.M., and Sclater, J.G. (1997) Digital isochrons of the world's ocean floor, Journal of Geophysical Research, v. 102, p. 3211-3214. Data: http://www-sdt.univ-brest.fr/~jyroyer/Agegrid/utig_report.html.

Müller, R.D., Royer, J.-Y., Cande, S. C., Roest, W.R., Maschenkov, S. (1999) New constraints on Caribbean plate tectonic evolution, Mann, P., ed., Sedimentary Basins of the World, v. 4, Elsevier, Amsterdam, p. 39-55.

Norton, I. O. (1995) Plate motions in the North Pacific: the 43 Ma non-event, Tectonics, v. 14, p. 1080-1094.

Norton, I. O. (2000) Global hotspot reference frames and plate motion, *in* Richards, M. A., Gordon, R. G., and van der Hilst, R. D., editors, The history and dynamics of global plate motions, American Geophysical Union Geophysical Monograph 121, p. 339-357.

Pilger, R. H. (2003a) Geokinematics: Prelude to Geodynamics, Springer-Verlag, Berlin, 338 p.

Press, W. H., Teukolsky, S. A., Vetterling, W. T., and Flannery B. P. (1992) Numerical Recipes in C: The Art of Scientific Computing, Second Edition, Cambridge University Press, Cambridge, England, 994 p.

Raymond, C. A , Stock, J. M., and Cande, S. A. (2000) Fast Paleogene motion of the Pacific hotspots from revised global plate circuit constraints, *in* Richards, M. A., Gordon,

R. G., and van der Hilst, R. D., editors, The history and dynamics of global plate motions, American Geophysical Union Geophysical Monograph 121, p. 359-375. Corrected parameters: http://www.gps.caltech.edu/~jstock/Raymond-et-al.Table1.corr.htm.

Sharp, W. D., and Clague, D. A. (2002) An Older, Slower Hawaii-Emperor Bend, EOS Transactions of the American Geophysical Union, v. 83, Fall Meeting Supplement, Abstract T61C-04.

Wilder, D. T. (2003), Relative motion history of the Pacific-Nazca (Farallon) plates since 30 million years ago, Masters Thesis (unpublished), University of South Florida, 94 p.

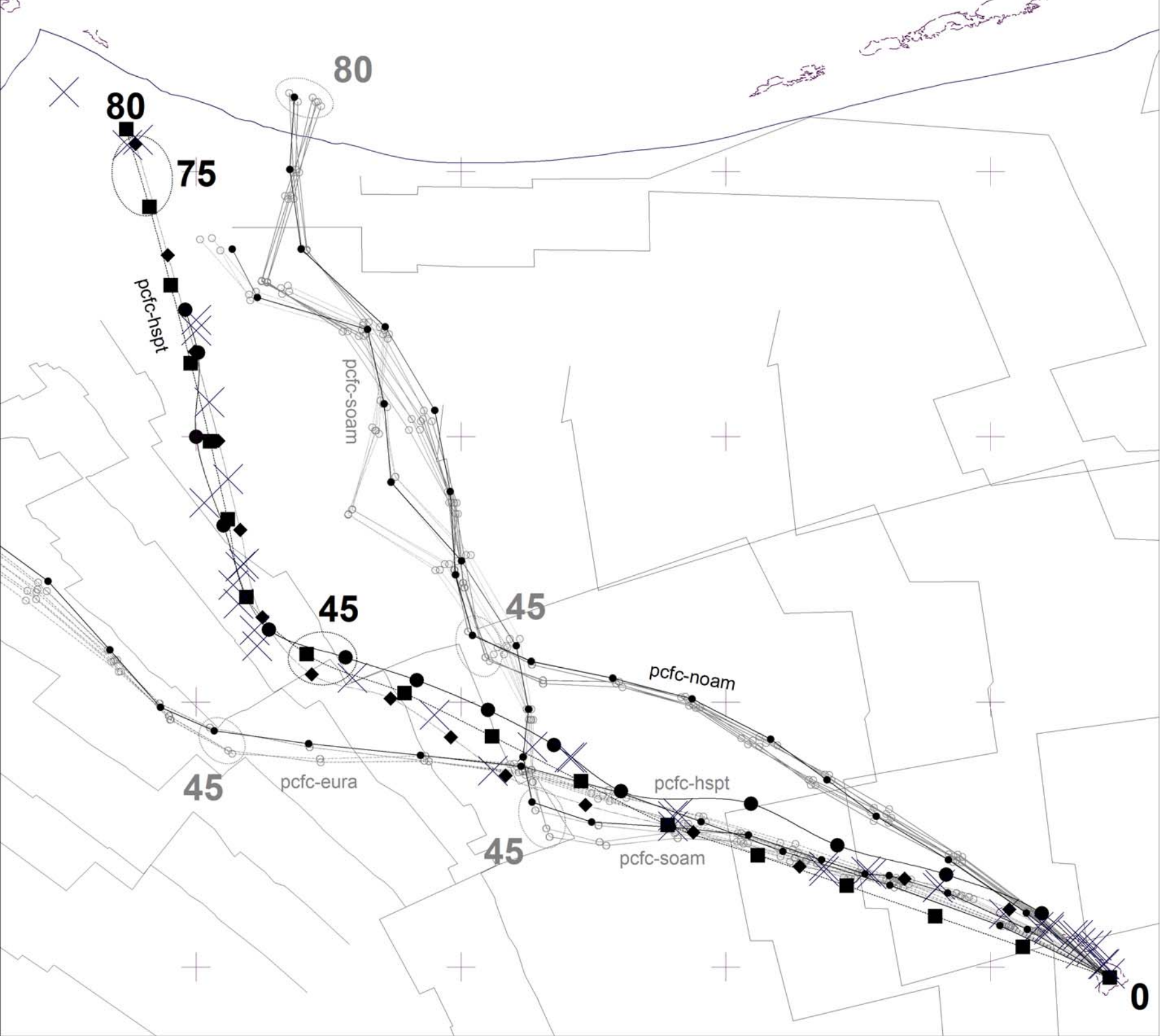
80
80
75
pcfc-hspt
pcfc-soam
45
45
pcfc-noam
45
pcfc-eura
pcfc-hspt
45
pcfc-soam
0

The Bend: Origin and Significance

Full Size Figures:

Figure 1. North central Pacific Ocean bathymetry (after Smith and Sandwell, 1999), with predicted locus of Pacific Plate relative to a fixed Hawaiian hotspot, calculated at 5 m.y. interval (after Raymond et al., 2000, corrected). Calculation methods are described in the Appendix (in the data repository).

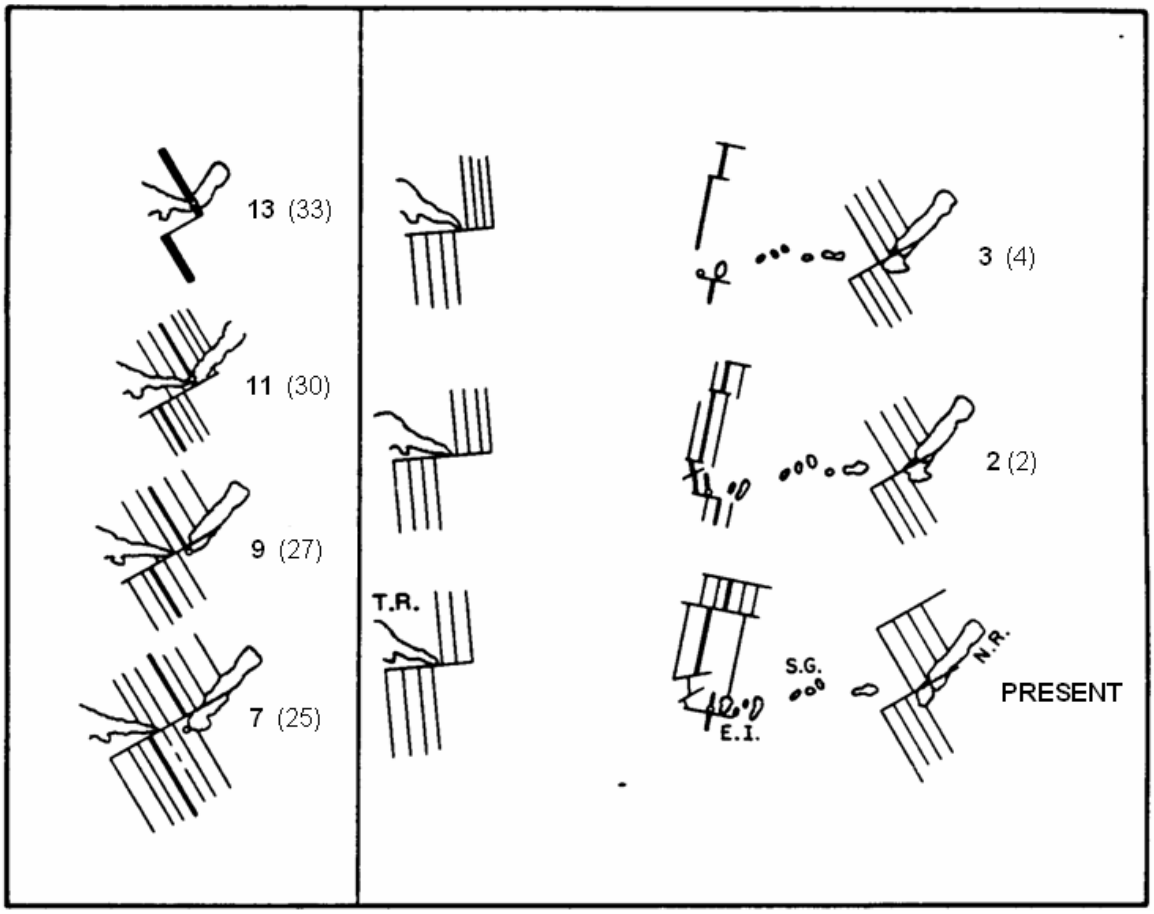

Figure 2. Schematic evolution of east central Pacific Ocean from magnetic isochron 13 to Present, based on plate reconstructions of Pilger and Handschumacher (1981). Note that the isochron-fracture zone reconstructions also result in juxtaposition of Tuamotu and Nazca ridges at the Pacific-Nazca (-Farallon) spreading center until isochron 11 time. This implies generation of the ridges by a melting anomaly beneath the spreading center (from at least isochron 21 to isochron 11 times). It is difficult to see how oblique propagating fractures could produce the “mirror-image” ridges without a sublithospheric melting anomaly.

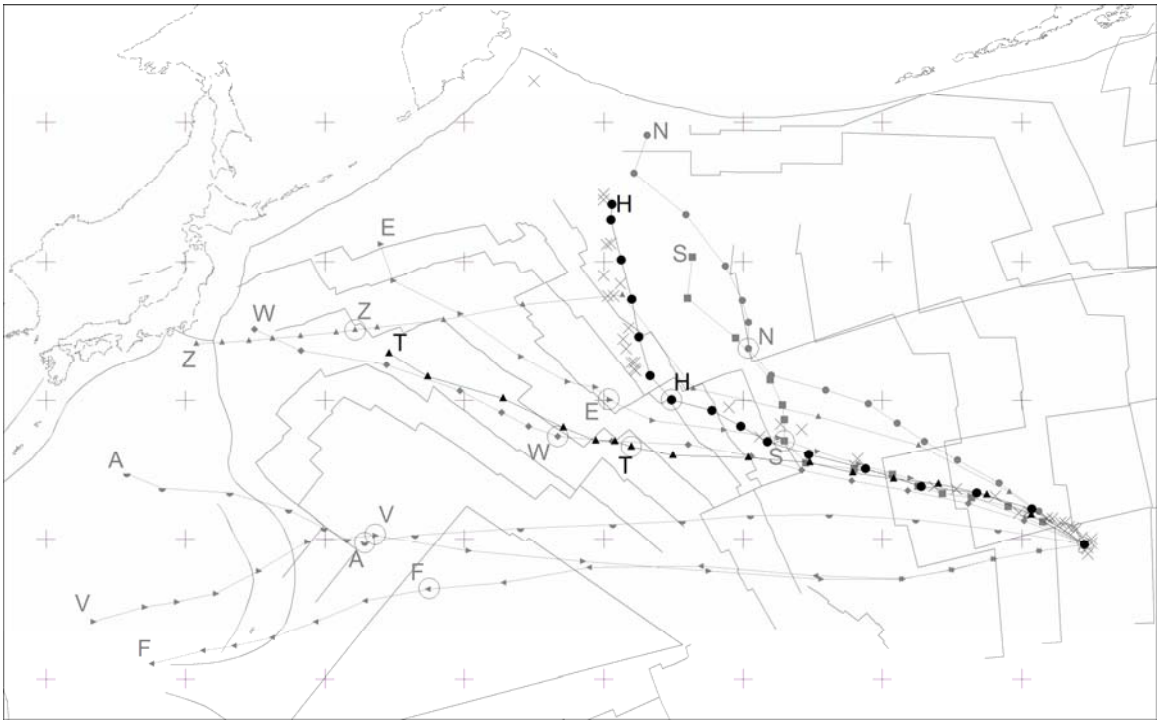

Figure 3. Loci of several plates and Hawaiian and Tristan (Atlantic-Indian Ocean) hotspot frames relative to a fixed Pacific plate – A: Australian, E: Eurasian, H: Hawaiian hotspot (model of Raymond et al., 2000), N: North American, S: South American, T: Tristan hotspot, W: West Antarctic, plus Pacific plate relative to adjacent (fixed) oceanic plates: F: Farallon, V: Vancouver, and Z: Nazca. Reconstructions at 5 m.y. intervals, calculated from Hawaii. Loci are constructed as if each plate or hotspot frame incorporated present day Hawaii and show the hypothetical path of the plate or frame relative to the fixed plate over the past 75 m.y. (Straight-line segments connect each calculated point). Reconstruction parameter sources are in Table 1 and plate circuits in Table 2, both in the repository. Calculation methods and parameters are in Appendices I and II in the data repository. Magnetic isochrons and plate boundaries are from Müller et al. (1997). Note changes in apparent plate motion between 45 and 50 Ma (that is, close to the age of the Hawaiian-Emperor bend), especially within the North and South American loci. Farallon and Vancouver loci also show slight changes. See Fig. 4 for a close-up of the younger portions of some of the critical loci.

Figure 4. Close-up of Figure 3, for Pacific plate motion relative to North American (NA) and South American (SA) plate and Hawaiian hotspot reference frames (with two more models shown). Reconstructions at 5 m.y. intervals, calculated from Hawaii. For Pacific-Hotspot, Harada and Hamano (2000): circles with fine dotted line; Norton (2000): squares with bold dotted line; Raymond et al. (2000): diamonds with solid line. Pacific-North American and South American: circles with solid lines. Note that the model for Harada and Hamano's parameters extends to only 70 Ma, not 75 Ma. Note subparallelism of North and South American loci with loci for the Hawaian hotspot, between ~25 and ~75 Ma (see also Norton, 1995), and, especially corresponding "bends" in the loci between 45 and 50 Ma.

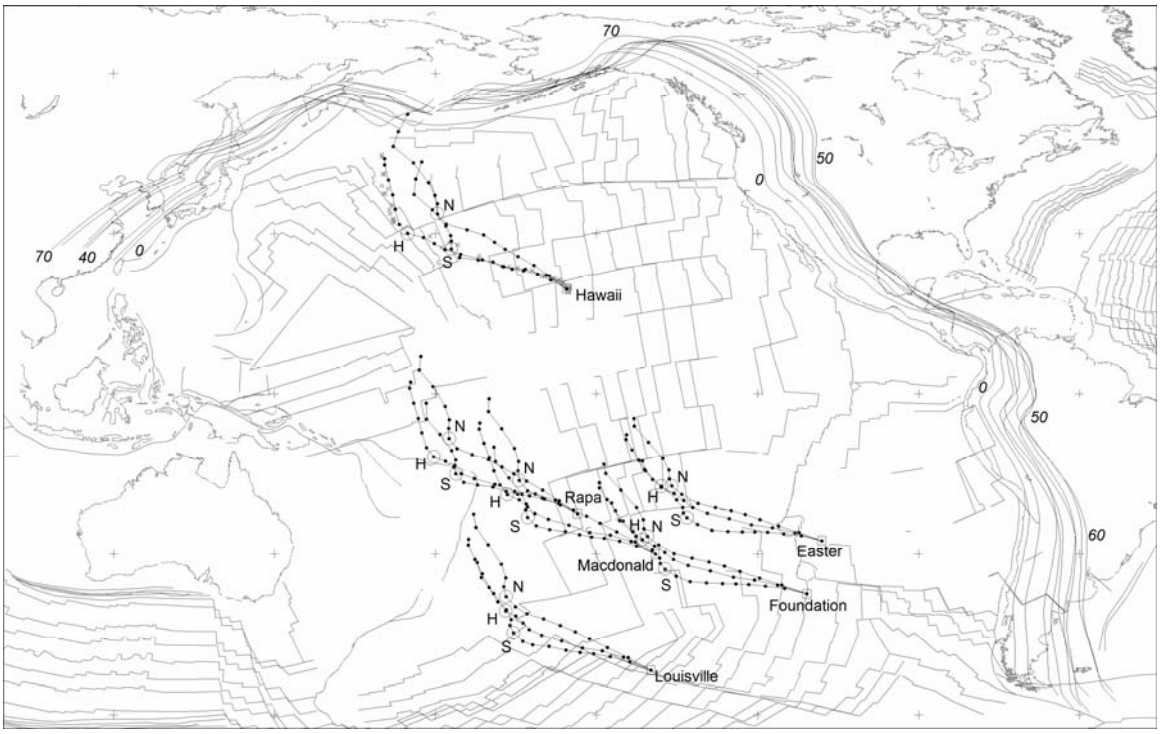

Figure 5. Reconstructed loci of North American (N), South American (S), and Pacific hotspots (H) relative to the Pacific plate, anchored at five postulated hotspots (Hawaii, Easter, McDonald, Rapa, and Louisville). Circled points are 45 Ma. Generalized continental, sublithospheric subduction margin of the circum-Pacific, restored to the Hawaiian hotspot frame; note clustering of restored margins, especially between 75 and 40 Ma. "X" indicates locations of dated samples from various hotspot traces. Magnetic isochrons and plate boundaries from Müller et al. (1997). Reconstruction sources, circuits, and parameters in Tables 1-3 in the data repository.

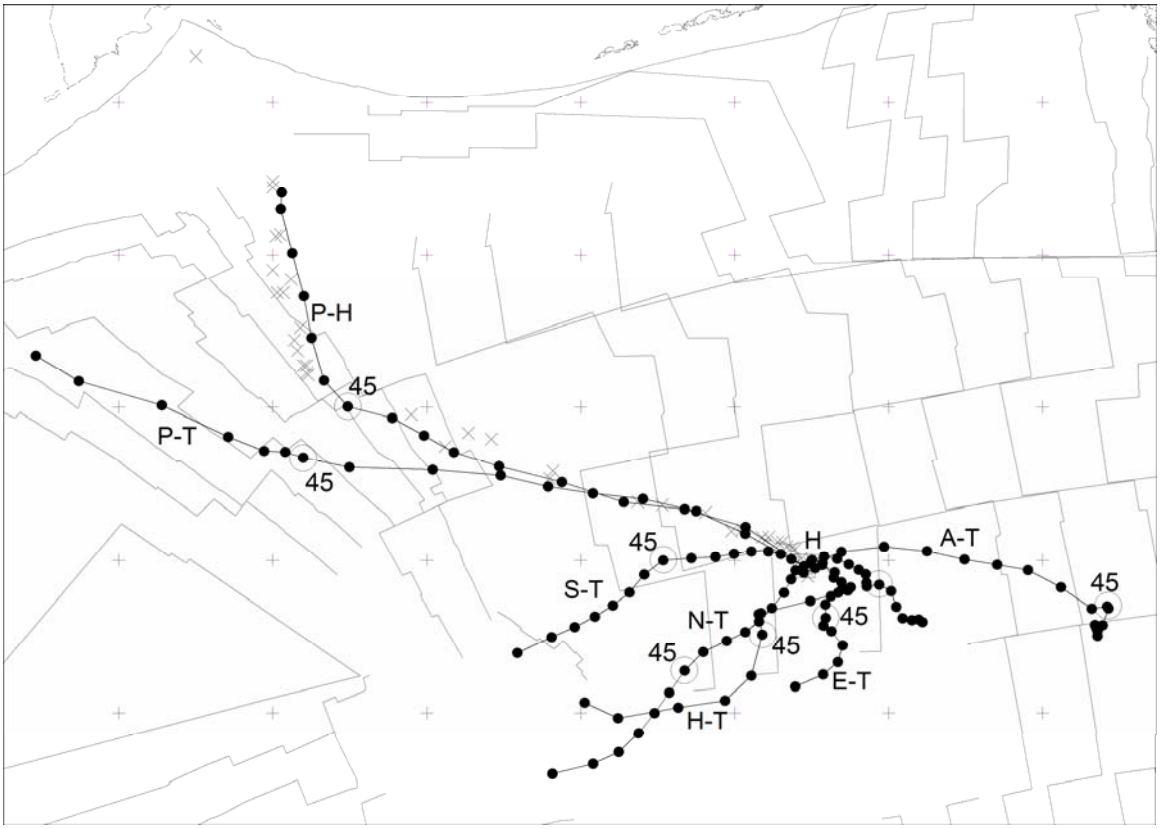

Figure 6. Loci of the several plates and Hawaiian hotspot relative to the Tristan (T) hotspot reference frames: A-T: Australian, E-T: Eurasian, H-T: Hawaiian hotspot, N-T: North American, P-T: Pacific, S-T: South American, W-T: West Antarctic, plus Pacific plate relative to Hawaiian hotspot (P-H). Reconstructions at 5 m.y. intervals, calculated from Hawaii. Loci represent hypothetic motion path of plate or frame relative to Tristan hotspot reference frame. Magnetic isochrons and plate boundaries from Müller et al. (1997). The discrepancy between the Pacific loci relative to the Hawaiian and Tristan hotspot reference frames is a measure of the relative independence of the two reference frames. Note subparallelism of South and North American-Tristan loci with Hawaiian-Tristan locus. This parallelism is the transformed equivalent to that in Pacific plate frame (Fig. 4).

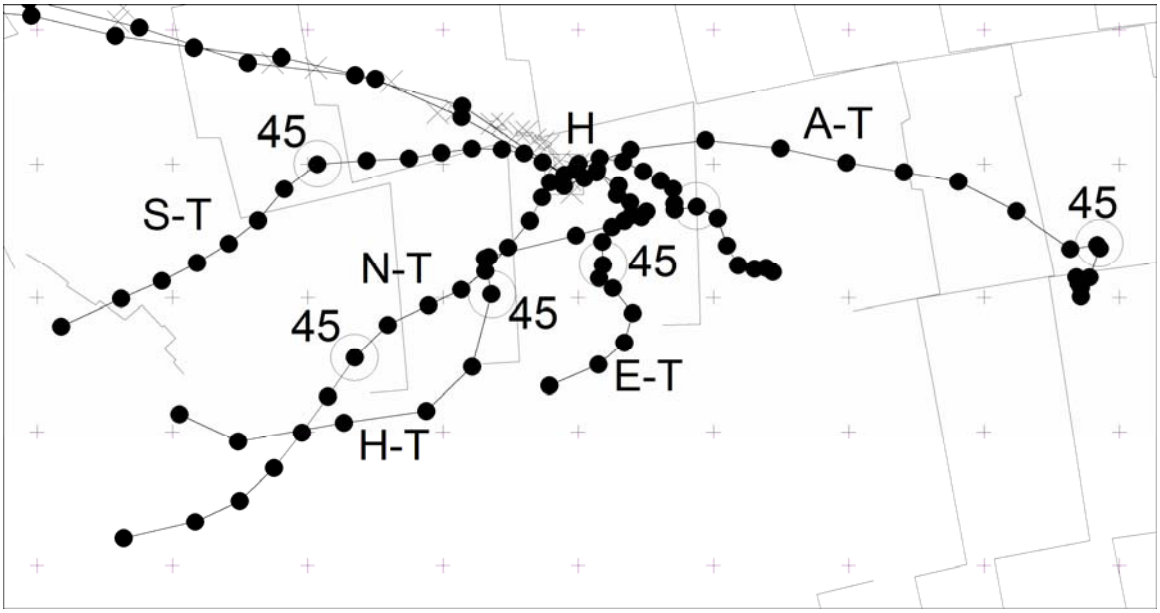

Figure 7. Close-up of Figure 6. Note subparallelism of Hawaiian-Tristan and North American-Tristan loci, between ~30 and 75 Ma.

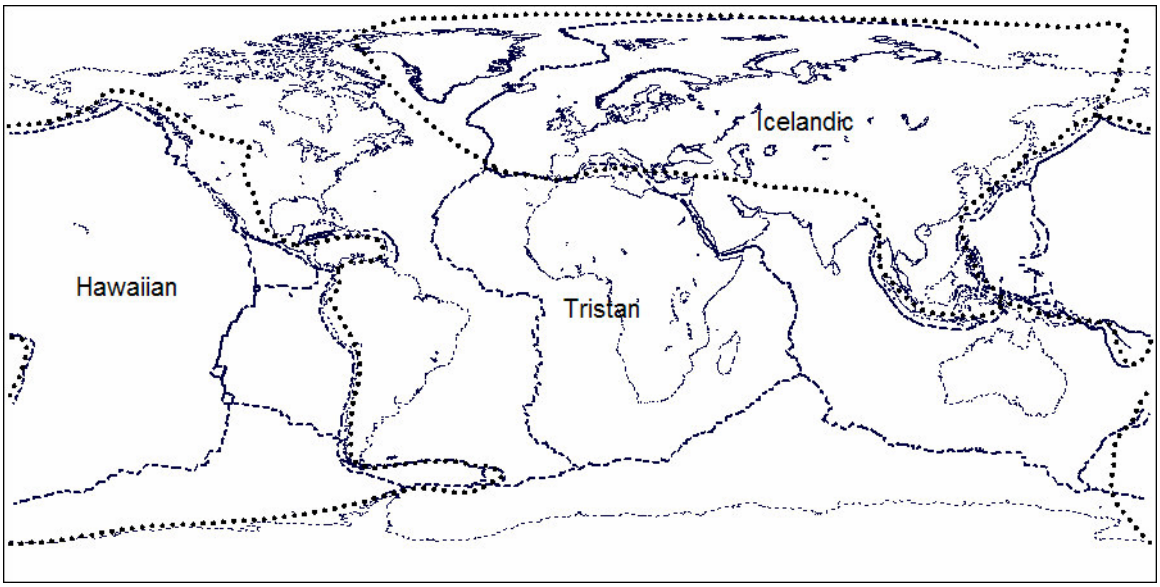

Figure 8. Proposed mesoplate boundaries (dotted polylines) modified from Pilger (2003a, b), to correspond with Liu et al.'s (2003) calculated high-stress boundaries (see also Liu, 2003; and Horowitz et al., 2001) and intraplate stress boundaries in western North America (Pilger, 2003a).

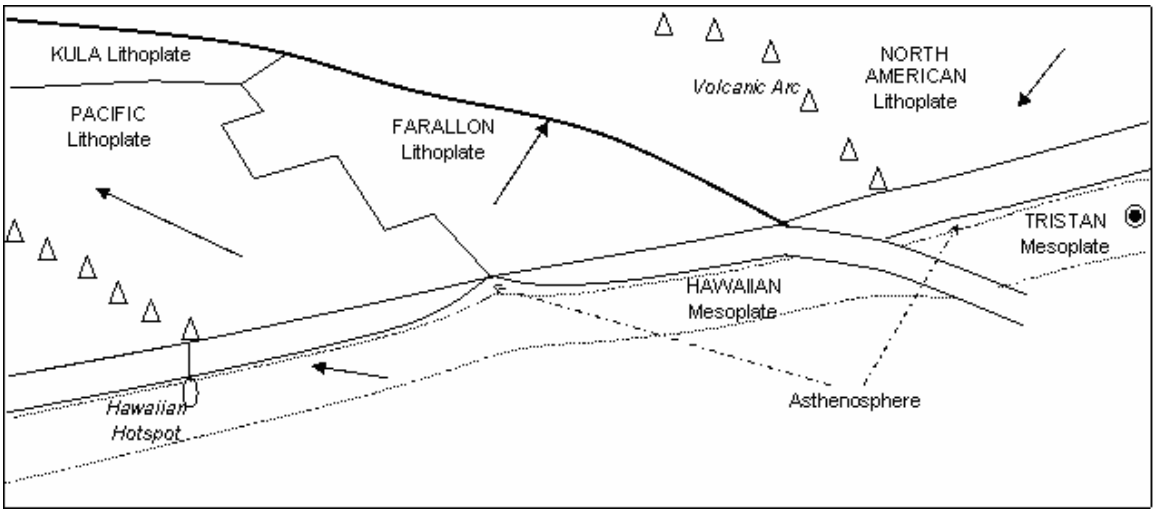

Figure 9. Schematic illustration of interaction of Pacific, Farallon, Kula, and North American lithoplates and Hawaiian and Tristan mesoplates (reference frames) in the early Cenozoic (~60 Ma). For convenience, Tristan mesoplate is fixed. Arrows indicate motion of Hawaiian mesoplate and lithoplates relative to Tristan.

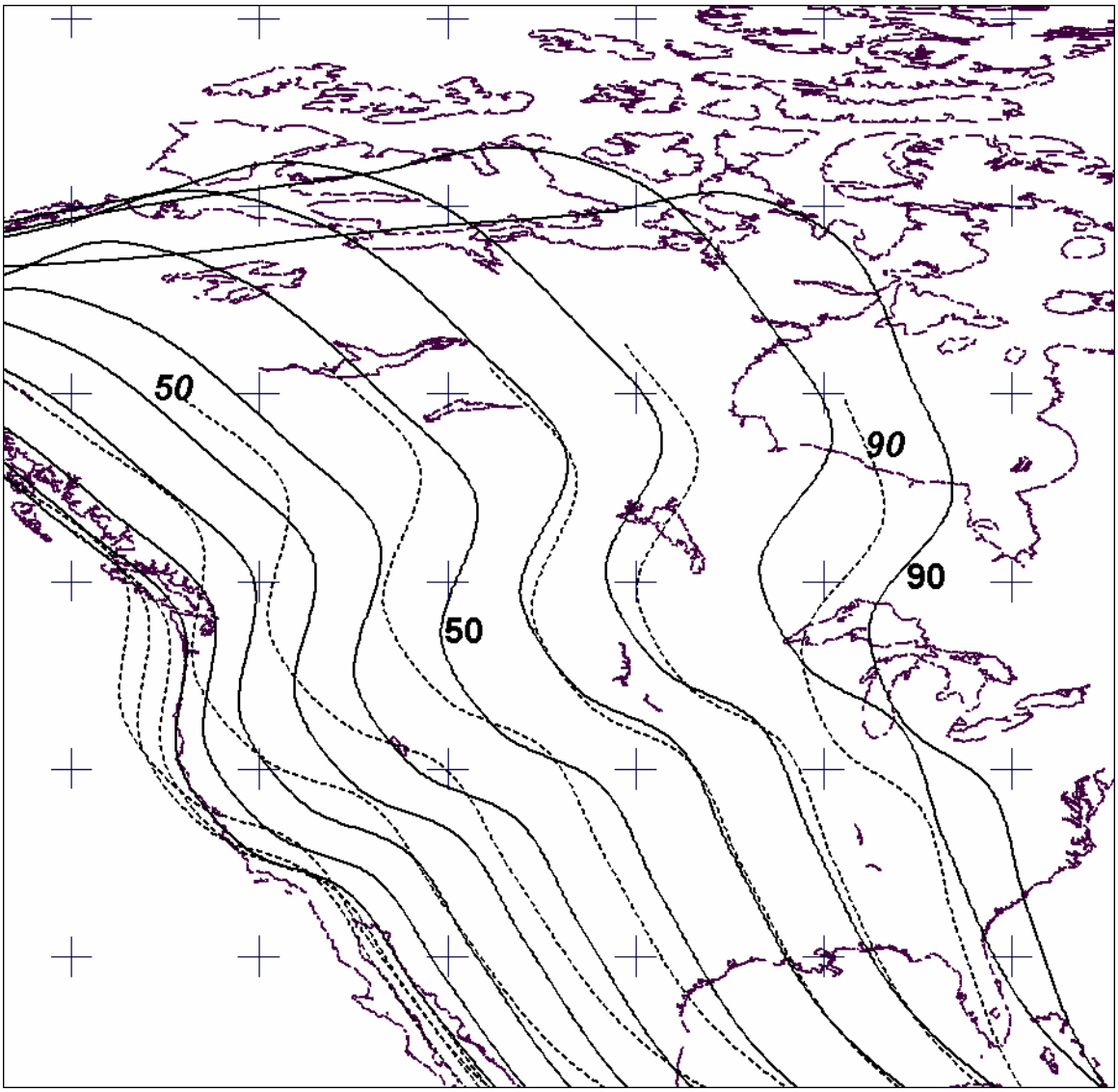

Figure 10. Reconstructions of the western margin of the North America at 10 m.y. intervals. Solid lines: North American lithoplate relative to the Tristan mesoplate (hotspot reference frame). Dashed lines: Hawaiian mesoplate relative to Tristan mesoplate. Note western migration of both reconstructed margins between ~75 and 30 Ma. This implies that relative motion of North America and the Hawaiian mesoplate during this time was minimal.

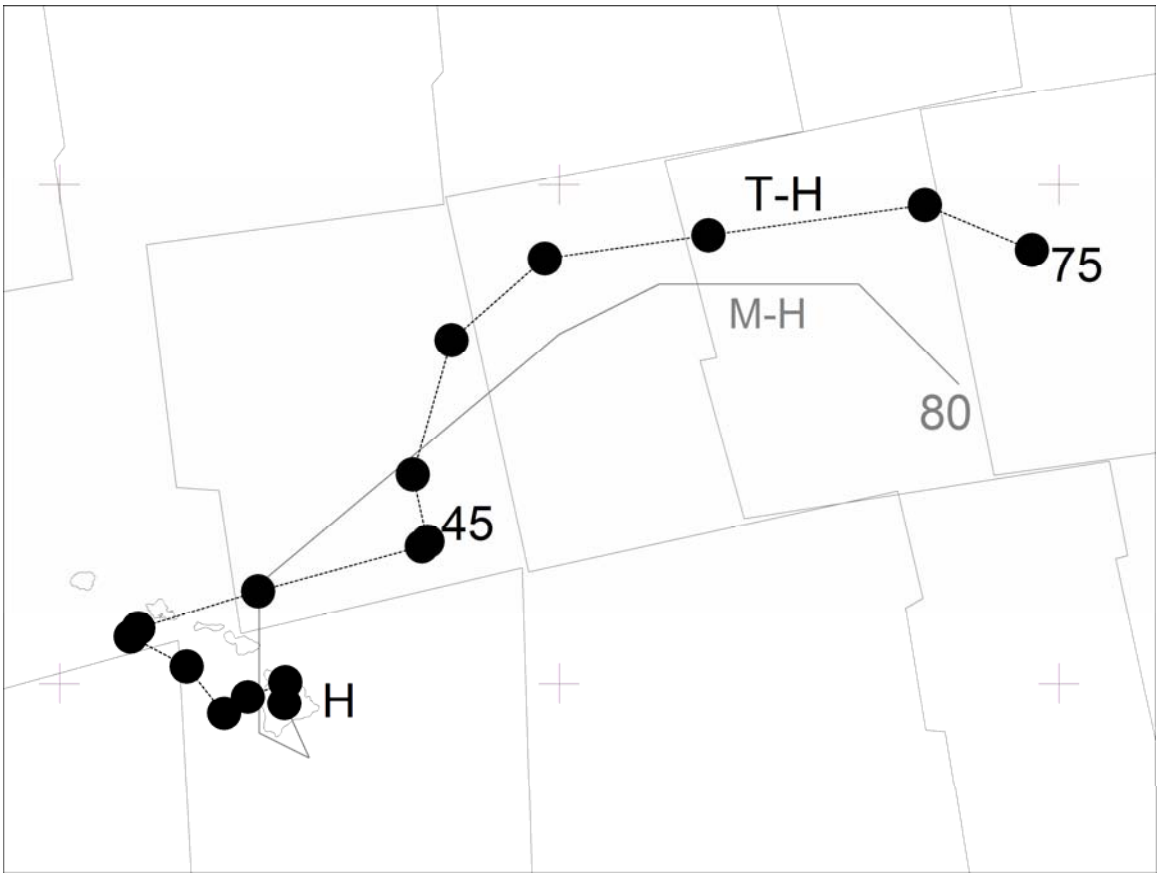

Figure 11. Loci of Hawaiian hotspot (H) relative to Tristan hotspot reference frame (T-H; dashed line and solid circles; this paper) and relative to the mean convective frame of O'Neill et al. (2005) (M-H: solid gray line, after their Fig. 17). Dates of end of loci (75 and 80) and intermediate point (45) in Ma. Latitude and longitude graticules are spaced at 10º intervals. As the published locus of O'Neill et al. (their Fig. 17) is shown in color gradations, precise ages cannot be shown.